Instituto Nacional de Astrofísica Óptica y Electrónica

Topological phenomena in active arrays

by

Phys. Erika Colín Ulloa

A dissertation submitted to in partial fulfillment of the requirements for the degree of

Master on Science with Major on Optics

Thesis Advisors:

Dr. J. Javier Sánchez Mondragón, INAOE

Dr. Demetrios Christodoulides, CREOL

February 2019

Tonantzintla, Puebla

Abstract

One of the most exciting developing fields in optics is the non-Hermitian topological photonics theory. This new field not only promises the understanding of the theoretical properties of non-Hermitian systems, but has also generated the possibility to develop more efficient materials. This new field have emerged from the merging of two frontiers research fields. One is the study of non-Hermitian Hamiltonians that has led to the study of the Parity-time symmetry theory (PT). Its application in Optics has originated diverse applications such as, invisibility metamaterials and metasurfaces and single mode selection, to selection a few. The second one is the application of topological concepts in physical systems.

The main objective of this work is to analyze a topological system with PT symmetry. The conditions where the PT symmetry and the topological properties are conserved in this theoretical model are determined.

The PT symmetry and the topology of a system have transition phases. In a PT symmetric system, it is called unbroken phase when the eigenvalues of the system are completely real and it is called broken phase when the symmetry is no longer fulfilled and generates imaginary eigenvalues. In the case of a topological system, the system presents the trivial topological phase and the non-trivial phase.

We will study the relation between the PT symmetry phases and the non-trivial phase of the topological system.

To achieve the main goal, the work is divided into two parts:

- An optical PT symmetric system made by two coupled microring resonators are analyzed. Through this model, the broken and unbroken PT phases are verified.
- Finally, through a finite SSH array composed of microrings resonators, we study the conditions to have PT symmetry in the system. The model analyzed has been taken from the work of M. Parto, et.al.,Phys. Rev. Lett. 120, 113901 (2018).

We corroborate that the system satisfies indeed the PT symmetry and topological conditions.

Resumen

Uno de los campos en desarrollo más emocionantes de la óptica es la fotónica topológica no Hermitiana. Este nuevo campo no solo promete la comprensión de las propiedades teóricas de los sistemas no Hermitianos, sino que también ha generado la posibilidad de desarrollar materiales más eficientes. Este nuevo campo ha surgido de la fusión de dos campos de investigación de frontera. Uno es el estudio de Hamiltonianos no Hermitianos que ha llevado al estudio de la teoría de la simetría de paridad-tiempo (PT). Su aplicación en óptica ha originado diversas aplicaciones, Tales como, invisibilidad en metamateriales y metasuperficies, selección de modo único, por ejemplo. El segundo es la aplicación de conceptos topológicos en sistemas físicos.

El objetivo principal de este trabajo es analizar la simetría PT en un arreglo topológico. Se determinarán las condiciones en las que la simetría PT y las propiedades topológicas se conservan en este modelo teórico.

La simetría PT y la topología de un sistema muestran fases de transición. En un sistema PT simétrico, se denomina fase no rota cuando los valores propios del sistema son completamente reales y fase rota cuando la simetría PT ya no se cumple y genera valores propios imaginarios. En el caso de un sistema topológico, el sistema presenta la fase topológica trivial y la fase no trivial, la última será analizada.

Estudiaremos la relación entre las fases de simetría PT y la fase no trivial del sistema topológico.

Para lograr el objetivo principal, el trabajo está dividido en dos partes:

• Estudio de un sistema óptico PT simétrico hecho por dos microanillos resonadores acoplados. A través de este modelo, se verificarán las fases PT no rota y rota.

• Finalmente, a través de un arreglo SSH formado por microanillos resonadores, se estudiarán las condiciones para que exista simetría PT. El modelo analizado ha sido tomado del trabajo de M. Parto, et.al., Phys. Rev. Lett. 120, 113901 (2018).

Corroboraremos que el sistema satisface tanto la simetría PT como el comportamiento topológico.

Contents

List of Figures

Preface

This thesis is related to the field of non-Hermitian topological photonics, by a theoretical study of two Parity-time symmetric systems. This work was done during my research stay in UCF-CREOL under the supervision of Dr. Demetrios Christodoulides with the final supervision of Dr. Sánchez Mondragón at INAOE.

The main objective of this work is to analyze a topological system with PT symmetry. This thesis is organized as follows:

Chapter 1 is a review of quantum theory and pseudo-Hermitian theory, to understand the context where the PT symmetric theory was developed.

Chapter 2 presents the PT Symmetry theory and its application to photonics.

Chapter 3 is a review of the band structure theory. This chapter will be useful to understand the topological phases of the system that will be described in Chapter 4.

Chapter 4 is an introduction of the topological properties in photonics. We will study the Su-Schrieffer-Heeger (SSH) model.

Chapter 5 presents the final results. In this chapter the PT symmetric-SSH array are analyzed. In this chapter a system of PT microring resonators is studied and the PT phases of the system will be shown. Then, the PT-SSH array is analyzed.

Chapter 6 presents the conclusions and future perspectives of the study.

Chapter 1

The theoretical background of Parity-Time symmetry

Abstract

This chapter is an introduction to the basis of the Parity-Time symmetric theory that will be studied in the Chapter 2.The main properties of quantum theory and the properties of the parity and time reversal operators are reviewed.

There are several proposals to build a theoretical basis for studying non-Hermitian Hamiltonians. One of these is the pseudo-Hermitian Hamiltonian theory. In this chapter, we briefly show the main features of this theory.

Introduction

The quantum theory is one of the most important theories in Physics, which, since its emergence, it has established its mathematical foundations in a rigorous way.

Such mathematical rigor, which ensures the conservation of probability and the existence of real eigenvalues, has led to the exclusion of non-Hermitian systems.

Several approaches like the one developed by Mostafazadeh[1], through the pseudo-Hermitian Hamiltonians theory, have been proposed that suggest the extension of the quantum theory.

[1] Mostafazadeh A., Phys. Rev. A, 87 (2013) 012103.

1.1 Quantum Theory

The quantum theory describes the behavior of a system, in a Hilbert space, associated with the wave function Ψ, fulfilling the Schrödinger equation:

$$i\hbar\frac{\partial\Psi}{\partial t}=\hat{H}\Psi \tag{1}$$

Where $\hbar$ is the Planck constant and $\hat{H}$ is the Hamiltonian operator $\hat{H}=\frac{\hat{p}^2}{2}+V\left(\hat{x}\right)$ that determines the energy eigenstates and the eigenvalues correspond to the energy levels, using the independent Schrödinger equation $H\left|E_n\right\rangle=E_n\left|E_n\right\rangle$. These energy eigenvalues are real numbers. $\hat{p}$, V and $\hat{x}$ correspond to the momentum eigenvector, potential and position eigenvector respectively.

In addition, the theory is stipulated under the following conditions[2]:

– Symmetry. If an operator $\hat{A}$ (unitary or anti-unitary) satisfies $\hat{A}^{\dagger}\hat{H}\hat{A}=\hat{H}$ it represents symmetry of the Hamiltonian $\hat{H}$. Then, $\hat{A}$ commutes with the Hamiltonian $\hat{H}$, $\left[\hat{A},\hat{H}\right]=0$. This means that the eigenstates of $\hat{H}$ are also eigenstates of $\hat{A}$.

– The Hamiltonian determines the time evolution giving by the time-dependent Schrödinger Equation $H\left|t\right\rangle=-i\frac{d}{dt}\left|t\right\rangle$ whose solution is $\left|t\right\rangle=\hat{U}\left|0\right\rangle$.Where $\hat{U}$, a unitary operator, is called unitary evolution operator.

– Unitarity must not be violated. Using the solution of the time-dependent solution, we have that the operator $\hat{U}$ is unitary if satisfies $\hat{U}^{\dagger}=\hat{U}^{-1}$ or $\hat{U}\hat{U}^{\dagger}=\hat{1}$.

[2] C. M. Bender, and S. Boettcher, "Real spectra in non-Hermitian Hamiltonians having PT symmetry," Phys. Rev. Lett. 80, 5243 (1998).

We have that that operator $\hat{U}$ preserves the norm with the time (probability is conserved) and this must be real and positive, $\left\langle \hat{U}\psi \middle| \hat{U}\varphi \right\rangle = \langle \psi | \varphi \rangle$.

However, these conditions exclude the use of complex Hamiltonians since they only establish the study of real and symmetric Hamiltonians. Because of this, the Hermiticity has been established as the indispensable condition for studying a physical system in quantum mechanics, this condition allows the use of complex Hamiltonians and guarantees the existence of real eigenvalues and the unitarity with time, two of the essential properties of the theory.

1.1.1 Parity and time reversal operators

Two of the most important operators in Quantum Theory are the parity $\hat{P}$ and the time reversal $\hat{T}$ operators. These operator acting on the dynamical variables $\hat{x}$ (the coordinate operator) and $\hat{p}$ (the momentum operator). The effect of each operator are defined as follows.

The Parity operator $\hat{P}$ is a spatial transformation whose effect is the reflection in position, this means:

$$\begin{aligned} &\hat{x} \to -\hat{x} \\ &\hat{p} \to -\hat{p} \\ &\langle \hat{x} \rangle \to -\langle \hat{x} \rangle \\ &\langle \hat{p} \rangle \to -\langle \hat{p} \rangle \\ &\langle x | \hat{P} | \psi \rangle = \psi(-x) \\ &\langle p | \hat{P} | \psi \rangle = \psi(-p) \end{aligned} \tag{2}$$

We have that $\hat{x}$ and $\hat{p}$ operators are transformed under spatial inversion by the rule:

$$\begin{aligned} &\hat{P}^{\dagger} \hat{x} \hat{P} = -\hat{x} \\ &\hat{P}^{\dagger} \hat{p} \hat{P} = -\hat{p} \end{aligned} \tag{3}$$

Where parity operator is unitary $\hat{P}^{\dagger}\hat{P}=\hat{1}$. In addition $\hat{P}$ is linear, considering $\left[\hat{x},\hat{p}\right]=i\hat{1}\hbar$, the operator satisfies $\hat{P}^{\dagger}i\hat{1}\hbar\hat{P}=i\hat{1}\hbar$.

We have that a Hamiltonian is P-invariant if satisfies the relation:

$$\hat{H}\left(\hat{x},\hat{p}\right)=\hat{H}\left(-\hat{x},-\hat{p}\right)\rightarrow\hat{P}^{\dagger}\hat{H}\hat{P}=\hat{H} \tag{4}$$

Where parity is conserved, $\left[\hat{P},\hat{H}\right]=0$

The effect of Time reversal operator $\hat{T}$ is the reversal of motion:

$$\begin{aligned} t &\rightarrow -t \\ \left\langle\hat{x}\right\rangle &\rightarrow \left\langle\hat{x}\right\rangle \\ \left\langle\hat{p}\right\rangle &\rightarrow -\left\langle\hat{p}\right\rangle \end{aligned} \tag{5}$$

Under the action of this operator, the rules of transformation are:

$$\begin{aligned} \hat{T}^{\dagger}\hat{x}\hat{T}&=\hat{x} \\ \hat{T}^{\dagger}\hat{p}\hat{T}&=-\hat{p} \end{aligned} \tag{6}$$

To find how the Time reversal operator $\hat{T}$ preserves the normalization of the wave function, with a time-independent Hamiltonian, the behavior of this operator will be studied.

Considering the time evolution of the function where $\hat{U}=e^{-i\hat{H}t/\hbar}$ is introduced as a unitary operator.

$$\left|\psi\left(t\right)\right\rangle=\hat{U}\left(t\right)\left|\psi\left(0\right)\right\rangle \tag{7}$$

Applying the action of $\hat{U}$ on a time reversed state and taking into account that $\hat{T}$ must preserve the norm of the wave function $\hat{T}^{\dagger}\hat{T}=\hat{1}$:

$$\begin{aligned}
&\hat{T}\left|\psi(t)\right\rangle = \hat{T}\hat{U}(t)\left|\psi(0)\right\rangle \\
&\left|\psi(-t)\right\rangle = \hat{T}\hat{U}(t)\hat{T}^{\dagger}\hat{T}\left|\psi(0)\right\rangle \\
&\left|\psi(-t)\right\rangle = \hat{T}\hat{U}(t)\hat{T}^{\dagger}\left|\psi(0)\right\rangle \\
&\Rightarrow \hat{T}\hat{U}(t)\hat{T}^{\dagger} = \hat{U}(-t)
\end{aligned} \tag{8}$$

This implies

$$\begin{aligned}
&\hat{T}\hat{U}(t) = \hat{U}(-t)\hat{T} \\
&\hat{T}i\hat{H} = -i\hat{H}\hat{T}
\end{aligned} \tag{9}$$

We have that $\hat{T}$ and $\hat{H}$ anti-commute, if $\hat{T}$ is unitary, this leads to negative energies:

$$\hat{H}\hat{T}\left|\psi_{E}\right\rangle = -\hat{T}\hat{H}\left|\psi\right\rangle = -E\hat{T}\left|\psi\right\rangle \tag{10}$$

To have $\left[\hat{T},\hat{H}\right] = 0$ and to preserve the commutation relation $\left[\hat{x},\hat{p}\right] = i\hbar$, we noticed that:

$$\hat{T}\left[\hat{x},\hat{p}\right] = \left[\hat{x},-\hat{p}\right] = -i\hbar \tag{11}$$

Because of the equation (11) we have that $\hat{T}$ must be an anti-unitary operator defined as:

$$\begin{aligned}
&\hat{T} = \hat{U}\hat{K} \\
&\Rightarrow \hat{T}i = -i\hat{T}
\end{aligned} \tag{12}$$

Where $\hat{K}$ is the complex conjugation operator.

Applying (12) in (9) and (11), we obtain:

$$\begin{aligned}
&\hat{T}i\hat{H} = -i\hat{T}\hat{H} = -i\hat{H}\hat{T} \\
&\Rightarrow \hat{T}\hat{H} = \hat{H}\hat{T} \\
&\hat{T}\left[\hat{x},\hat{p}\right] = -i\hbar \\
&\Rightarrow \hat{\mathrm{T}}\mathrm{i}\left|\alpha\right\rangle = -i\left|\alpha\right\rangle
\end{aligned} \tag{13}$$

Because the properties of anti-unitary operators $\left\langle \hat{T}\psi \middle| \hat{T}\varphi \right\rangle = \langle \psi | \varphi \rangle^*$, we have that the Time reversal operator exchanges initial and final states.

Taking into account the last property, we obtain the time reversal rule for the wave function:

$$\langle x | \hat{T} \left| \psi(-t) \right\rangle = \left\langle \psi(-t) \middle| x \right\rangle \Rightarrow \hat{T}\psi(x,t) = \psi^*(x,-t) \tag{14}$$

To find the rule for the Hamiltonian $\hat{H}(\hat{x},\hat{p})$, we have:

$$\hat{T}^\dagger \hat{H}(\hat{x},\hat{p})\hat{T} = \hat{H}^*\left(\hat{T}^\dagger \hat{x}\hat{T}, \hat{T}^\dagger \hat{p}\hat{T}\right) = \hat{H}^*(\hat{x},-\hat{p}) \tag{15}$$

This means that a Hamiltonian will be $\hat{T}$ invariant if:

$$\hat{H}(\hat{x},\hat{p}) = \hat{H}^*(\hat{x},-\hat{p}) \tag{16}$$

1.2 Pseudo-Hermitian Hamiltonians

A Hamiltonian $\hat{H}$, in the Hilbert space, is pseudo-Hermitian if satisfies the definition:

$$\hat{H}^\dagger = \hat{A}\hat{H}\hat{A}^{-1} \tag{17}$$

Where $\hat{A}$ is a Hermitian operator:

$$\langle \psi(t), A\psi(t) \rangle = \langle \psi(0), A\psi(0) \rangle \tag{18}$$

We have that $\hat{A}$ is not unique, if the Hamiltonian satisfies the equation (17) for a specific operator $\hat{A}$, will be called A-pseudo-Hermitian.

For this Hamiltonians, the evolution is not unitary and the norm is not conserved in the same way that the Hermitian Hamiltonians.

We will have that the eigenfunctions are not orthogonal. To show this property, equation (1) is multiplied by $\langle\psi_n|$ from the left and multiplying multiplying by $|\psi_k\rangle$ the Hermitian conjugate of (1) and, we obtain:

$$\begin{aligned} i\hbar\langle\psi_n|\frac{\partial|\psi_k\rangle}{\partial t} &= \langle\psi_n|\hat{H}|\psi_k\rangle \\ -i\hbar\frac{\partial\langle\psi_n|}{\partial t}|\psi_k\rangle &= \langle\psi_n|\hat{H}^\dagger|\psi_k\rangle \end{aligned} \tag{19}$$

We have that:

$$i\hbar\left(\langle\psi_n|\frac{\partial|\psi_k\rangle}{\partial t}+\frac{\partial\langle\psi_n|}{\partial t}|\psi_k\rangle\right)=\langle\psi_n|\hat{H}-\hat{H}^\dagger|\psi_k\rangle=i\hbar\frac{\partial\langle\psi_n|\psi_k\rangle}{\partial t} \tag{20}$$

where $\langle\psi_n|\psi_k\rangle$ establishes a pseudo inner product and $\hat{H}$ is Hermitian under this condition. This means:

$$\langle\psi_n|\psi_k\rangle_A := \langle\psi_n|\hat{A}\psi_k\rangle \tag{21}$$

$$\langle\psi_n,a|\psi_k,b\rangle=\delta_{nk}\delta_{ab} \tag{22}$$

$$\sum_{nk}|\psi_n\rangle\langle\psi_k|=\sum_{nk}|\psi_k\rangle\langle\psi_n|=1 \tag{23}$$

Where *a* and *b* are degeneracies labels. In this thesis will be considered only the non-degenerate case, the equation (23) appears without degeneracies.

By definition, the energies of a pseudo-Hamiltonian are:

$$\begin{aligned} \hat{H}|\psi_n\rangle &= E_n|\psi_n\rangle \\ \hat{H}^\dagger|\psi_k\rangle &= E_n{}^*|\psi_k\rangle \end{aligned} \tag{24}$$

In a pseudo-Hermitian Hamiltonian we have that the energy values may be complex.

1.2.1 Expectation values

Because the norm $N(t) \equiv \langle \psi(t) | \psi(t) \rangle$ of a pseudo-Hermitian Hamiltonian is not conserved, it is assumed the initial condition N(0)=1. The rate of the norm is defined by equation (20).

To know how this affect the expectation values of the pseudo-Hermitian Hamiltonian, we use the norm expression for a linear operator $\hat{A}$:

$$\langle \hat{A} \rangle_t = \frac{\langle \psi(t) | \hat{A} | \psi(t) \rangle}{\langle \psi(t) | \psi(t) \rangle} \tag{25}$$

Obtaining the change of the expectation value of $\hat{A}$:

$$\begin{aligned} \frac{\partial}{\partial t} \langle \hat{A} \rangle_t &= \frac{\partial}{\partial t} \frac{\langle \psi(t) | \hat{A} | \psi(t) \rangle}{\langle \psi(t) | \psi(t) \rangle} \\ &= \frac{\left(\frac{\partial}{\partial t} \langle \psi(t) | \hat{A} | \psi(t) \rangle \right) \langle \psi(t) | \psi(t) \rangle - \left(\frac{\partial}{\partial t} \langle \psi(t) | \psi(t) \rangle \right) \langle \psi(t) | \hat{A} | \psi(t) \rangle}{\langle \psi(t) | \psi(t) \rangle^2} \end{aligned} \tag{26}$$

Using (20)

$$\frac{\partial}{\partial t} \langle \hat{A} \rangle_t = \frac{1}{i\hbar} \frac{\langle \psi(t) | \hat{A}\hat{H} - \hat{H}^\dagger \hat{A} | \psi(t) \rangle \langle \psi(t) | \psi(t) \rangle - \langle \psi(t) | \hat{H} - \hat{H}^\dagger | \psi(t) \rangle \langle \psi(t) | \hat{A} | \psi(t) \rangle}{\langle \psi(t) | \psi(t) \rangle^2} \tag{27}$$

Applying (17) in the form: $\hat{A}\hat{H} = \hat{H}^\dagger \hat{A}$

$$-\frac{\partial}{\partial t} \langle \hat{A} \rangle_t = \frac{\langle \hat{A} \rangle}{\langle \psi(t) | \psi(t) \rangle} \frac{\partial}{\partial t} \langle \psi(t) | \psi(t) \rangle \tag{28}$$

Taking into account the initial condition $\langle \psi(0) | \psi(0) \rangle = 1$, we have:

$$\left\langle \hat{A} \right\rangle_t = \frac{\left\langle \hat{A} \right\rangle_0}{\left\langle \psi(t) \middle| \psi(t) \right\rangle} \tag{29}$$

This means that the expectation value in a pseudo-Hermitian Hamiltonian is rescaled.

1.2.2 Involution operators

In every diagonalizable (21-23) pseudo-Hermitian Hamiltonian $\hat{H}$ exist a symmetry by a linear involution $\hat{S}$ and a symmetry generated by an antilinear involution $\hat{\Sigma}$[1]:

$$\begin{aligned} &\left[\hat{H}, \hat{S}\right] = \left[\hat{H}, \hat{\Sigma}\right] = 0 \\ &\hat{S}^2 = \hat{\Sigma}^2 = 1 \quad (\textit{involution}) \end{aligned} \tag{30}$$

Chapter 2

Parity-Time Symmetry Theory

Abstract

In this chapter, the main features of the parity-time (PT) symmetry theory are studied. We will see that if a non-Hermitian system has PT symmetry, it will keep real eigenvalues under specific conditions in the potential. It will also be shown that if these conditions are modified, the system will generate purely imaginary eigenvalues (PT symmetry broken). In addition, it will be shown that PT theory is a particular case of the Pseudo-Hermitian Theory.

Introduction

Hamiltonians with non-real eigenvalues for a long time were not studied because they did not satisfy one of the strongest conditions in quantum theory, the Hermiticity, that is established as: $H = H^{\dagger}$. However, during the decades of 1970 to 1990[3], several scientists realized that some non-Hermitian Hamiltonians might have real eigenvalues. These previous works contributed to the creation in 1997 of the PT symmetry theory, proposed by C. M. Bender and S. Boettcher. They proposed a way to replace the condition of Hermiticity by the condition space-time reflection symmetry (PT symmetry).

Nowadays, the application of this theory in optics has been very successful, generating the discovering of new phenomena.

[3] C M. Bender, "Introduction to PT-symmetric quantum theory". Contemp. Phys. 46 277 (2005).

2.1 Parity-Time operator

In general, the Hamiltonian $\hat{H} = \frac{\hat{p}^2}{2m} + V(\hat{x})$ associated with a complex potential $V(\hat{x})$ is parity–time symmetric ($\hat{P}\hat{T}$) if $\hat{H}$ satisfies the relation defined as follows[3]:

$$\hat{H}(\hat{x},\hat{p})\hat{P}\hat{T} = \hat{P}\hat{T}\hat{H}(\hat{x},\hat{p}) \tag{31}$$

Considering (4) and (16), we have that the transformation of the Hamiltonian under the $\hat{P}\hat{T}$ operator is:

$$\hat{P}\hat{T}\hat{H}(\hat{x},\hat{p}) = \hat{H}^*(-\hat{x},\hat{p}) \tag{32}$$

Because $\hat{P}\hat{T}$ is not linear, the eigenstates of $\hat{H}$ may or may not be eigenstates of $\hat{P}\hat{T}$.

Applying (31) to $\hat{H} = \frac{\hat{p}^2}{2m} + V(\hat{x})$, we have:

$$\begin{aligned}
&\left(\frac{\hat{p}^2}{2} + V(\hat{x})\right)\hat{P}\hat{T}\Psi(\hat{x}) = \hat{P}\hat{T}\left(\frac{\hat{p}^2}{2} + V(\hat{x})\right)\Psi(\hat{x}) \\
&\left(\frac{\hat{p}^2}{2} + V(\hat{x})\right)\Psi^*(-\hat{x}) = P\left(\frac{\hat{p}^2}{2} + V^*(\hat{x})\right)\Psi^*(\hat{x}) \\
&\left(\frac{\hat{p}^2}{2} + V(\hat{x})\right)\Psi^*(-\hat{x}) = \left(\frac{\hat{p}^2}{2} + V^*(-\hat{x})\right)\Psi^*(-\hat{x}) \\
&\Rightarrow V(\hat{x}) = V^*(-\hat{x})
\end{aligned} \tag{33}$$

This means that a necessary condition to have PT symmetry is that $V(\hat{x})$ satisfies the relation: $V(\hat{x}) = V^*(-\hat{x})$.

2.2 Real eigenvalues condition

The eigenvalues of a PT system with Hamiltonian $\hat{H}$ will be real if the eigensolutions are PT symmetric:

$$\psi_n = \hat{P}\hat{T}\psi_n \tag{34}$$

$$\hat{H}\psi_n = E_n\psi_n \tag{35}$$

Applying the $\hat{P}\hat{T}$ operator in (35), using (34) and the fact that $\hat{P}\hat{T}$ is antilinear:

$$\begin{aligned} &\hat{P}\hat{T}\hat{H}\psi_n = \hat{P}\hat{T}E_n\psi_n \\ &\Rightarrow \\ &\hat{P}\hat{T}\hat{H}\psi = \hat{H}\psi \\ &\hat{P}\hat{T}E_n\psi_n = E^*{}_n\psi_n \end{aligned} \tag{36}$$

We have:

$$\begin{aligned} &\hat{H}\psi_n = E_n^*\psi_n \\ &\Rightarrow E_n = E_n^* \end{aligned} \tag{37}$$

The equation (37) represents that the PT symmetry of ψ_n is a sufficient condition to have real eigenvalues.

2.2.1 Broken and unbroken PT symmetry

The condition showed in (37) is not a generalization for the eigensolutions of the PT system.

If every eigensolution of a PT -symmetric Hamiltonian is also an eigensolution of the PT operator, we will have that the PT symmetry of H is unbroken and all the eigenvalues will be real.

But, if some of the eigensolutions do not satisfy this condition, we will have that PT symmetry of H is broken and their eigenvalues will be complex.

2.3 PT symmetry and Pseudo-Hermitian Theory

The $\hat{P}$ and $\hat{T}$ operators satisfies the condition (30):

$$\begin{aligned} &\left[\hat{H},\hat{S}\right]=\left[\hat{H},\hat{P}\right]=0 \\ &\left[\hat{H},\hat{\Sigma}\right]=\left[\hat{H},\hat{T}\right]=0 \\ &\hat{P}^2=\hat{T}^2=1 \end{aligned} \tag{38}$$

Then, the operators satisfies the condition (17):

$$\begin{aligned} &\hat{H}^\dagger=\hat{P}\hat{H}\hat{P}=\hat{T}\hat{H}\hat{T} \\ &\Rightarrow \hat{P}\hat{T}\hat{H}=\hat{H}\hat{P}\hat{T} \\ &\therefore\left[\hat{P}\hat{T},\hat{H}\right]=0 \end{aligned} \tag{39}$$

The pseudo-Hermiticity condition coincides with the PT-symmetry condition, so that the PT-symmetry is considered a class of Pseudo-Hermitian systems.

Chapter 3

The Band Structure Theory

Abstract

This chapter is an important introduction to understand the topological behavior of a crystal, through its band diagram. In this thesis the Su-Schrieffer-Heeger (SSH) model will be studied, because of that, the band diagram of this model will be shown.

Introduction

The band theory was created in 1927 to simplify the study of the electronic transport in solids, where it yield diagrams that show the energy levels allowed for a crystalline material. Currently it is a widely used method since the electrical and optical properties of crystals can be determined, characterized by their band structures[4].

A band structure is a 2D representation of the energies of the orbitals in a crystalline material versus the wavevector k; it can show if a material is metallic, semi-metallic or insulating.

[4] P. Hofmann, "Solid State Physics", Wiley-VCH, Weinheim, 2008.

3.1 Band Structures

Considering a 1D Hamiltonian of an electron, with periodic potential V(x) and translational period. Defining the operator T_R acting on a function $f(x)$ as[5]: $T_R f(x) = f(x+R)$ and the function (Bloch function) $\phi_k(x) = \exp(ikx)u_k(x)$ where $u_k(x)$ is a function with the same periodicity as V(x), $u_k(x+nR) = u_k(x)$ for all integers n. We have:

$$T_R\phi_k(x) = \phi_k(x+R) = \exp(ikR)\phi_k(x) \tag{40}$$

From (40) we can see that the eigenfunctions of the Hamiltonian can be expressed as the eigenfunctions of T_R , so that an eigenfunction $\phi(x)$ of the Hamiltonian can be expressed as:

$$\phi(x) = \sum_k A_k\phi_k(x) = \sum_k A_k \exp(ikx)u_k(x) \tag{41}$$

The wave functions can be enumerated by the constants k, so if the energy of the electrons is plotted vs k, the band structure of the crystal will be obtained. Due to the conditions of symmetry, the k is not unique, so to simplify the study, Brillouin first zone is defined, in a 3D crystal, as the unitary region of reciprocal to the area defined in the interval $[-\pi/R, \pi/R]$, where Γ,M y X means the center, corner and face of the reciprocal lattice, respectively. Where the real lattice is the minimum structure from which the periodicity of structure originates.

As an example, figure 1 shows the Brillouin zone of a square lattice, as can be seen, the blue area corresponds to the Brillouin zone[5].

[5] Joanopoulus J. D., R. D. Meade, J. N. Winn. Photonic Crystals: Moldingthe Flow of Light, Princeton, NJ, Princeton University Press, 1995.

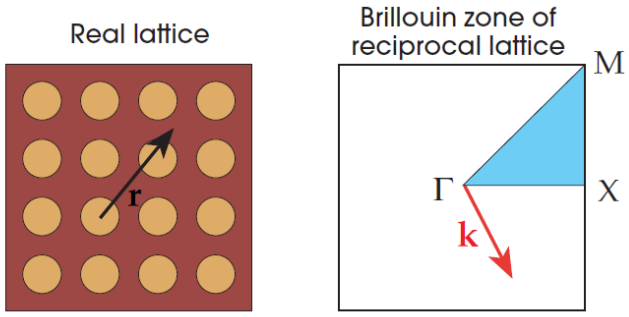

Figure 1. Left: Square lattice, Right: Brillouin zone[5].

One of the periodic lattices that will be used in this work is the Su-Schrieffer-Heeger (SSH) model, whose more detailed deduction is shown below.

3.2 The Su-Schrieffer-Heeger (SSH) Lattice

The Su-Schrieffer-Heeger (SSH) model consists of electrons located in a one-dimensional chain of N unit cells. Figure 2:

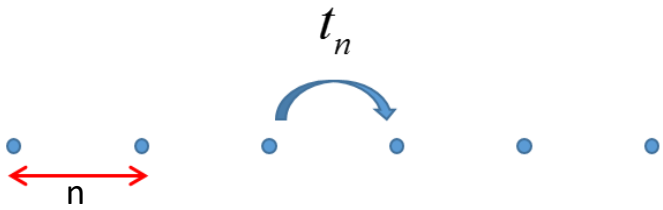

Figure 2. SSH lattice representation.

The simplest Hamiltonian for this model is the following[6]:

$$\hat{H} = -\sum_{n=1}^{N}\left(t\hat{c}_n^{\dagger}\hat{c}_{n+1} + h.c.\right) + \sum_{n=1}^{N} V_n \hat{c}_n^{\dagger}\hat{c}_n \qquad \text{with} \quad N = \sum_{n=1}^{N}\hat{c}_n^{\dagger}\hat{c}_n \tag{42}$$

[6] Asbóth J.K., Oroszlány L., Pályi A. (2016) The Su-Schrieffer-Heeger (SSH) Model. In: A Short Course on Topological Insulators. Lecture Notes in Physics, vol 919. Springer, Cham

Where h.c. means the Hermitian conjugate, $\hat{c}$ is the creation or annihilation operator and t means the position amplitude.

Considerations:

- One particle per unit cell
- Translational symmetry
- Same spacing t between particles.

Writing in the diagonalized form:

$$\hat{H} = \sum_k E(k)\hat{c}_k^\dagger \hat{c}_k \quad \text{with} \quad \hat{c}_n^\dagger = \frac{1}{\sqrt{N}}\sum_k e^{-ikna}\hat{c}_k^\dagger \tag{43}$$

Because V_nN is constant, the Hamiltonian takes the following form:

$$H = -t\left(\frac{1}{\sqrt{N}}\sum_k^N e^{-ikna}c_k^\dagger\right)\left(\frac{1}{\sqrt{N}}\sum_{k'}^N e^{ik'(n+1)a}c_{k'}\right) - t^*\left(\frac{1}{\sqrt{N}}\sum_k^N e^{-ik(n+1)a}c_k^\dagger\right)\left(\frac{1}{\sqrt{N}}\sum_{k'}^N e^{ik'na}c_{k'}\right)$$

$$H = -\sum_k \left(te^{ika} + t^* e^{-ika}\right)c_k^\dagger c_k = \sum_k E(k)c_k^\dagger c_k \tag{44}$$

$$\therefore E(k) = -t(2\cos ka)$$

Figure 3 shows the Band structure of SSH model with same value t between particles.

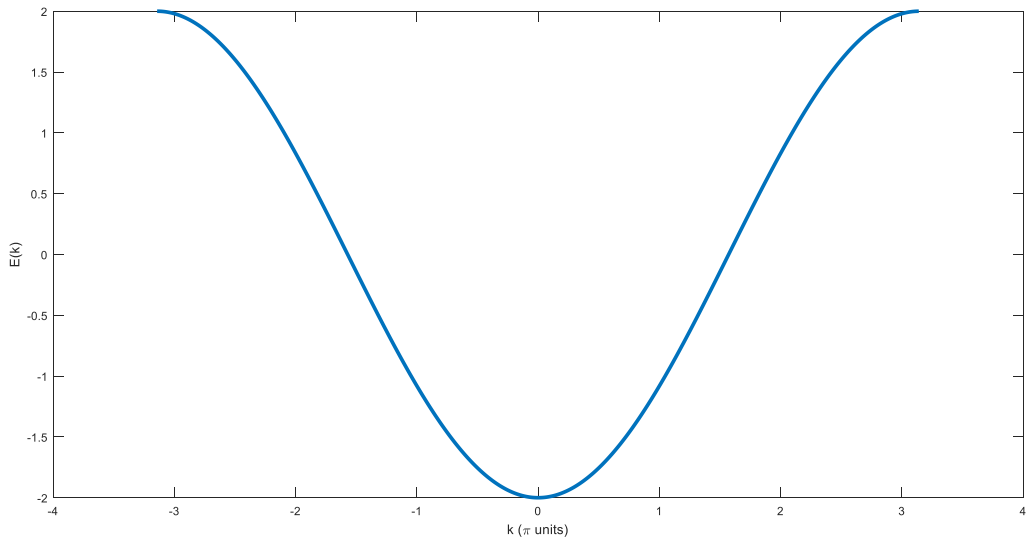

Figure 3. Eigen-energies SSH model with same t.

In general, the spacing t can be different from each other, considering t1 ≠ t2, we have the Hamiltonian:

$$H=\sum_{n=1}^{N}\left(v_n c_{n,1}^{\dagger}c_{n,2}+w_n c_{n,2}^{\dagger}c_{n+1,1}+h.c.\right)$$

$$\textit{defining}\quad c_n^{\dagger}=\left(c_{n,1}^{\dagger},c_{n,2}^{\dagger}\right)=\left(c_{2n-1}^{\dagger},c_{2n}^{\dagger}\right),\ \text{we have}\quad H=\sum_{m,n=1}^{N}c_m^{\dagger}H_{mn}c_n \tag{45}$$

Therefore, we obtain:

$$c_n^{\dagger}H_{nn}c_n=\begin{pmatrix}c_{n,1}^{\dagger} & c_{n,2}^{\dagger}\end{pmatrix}\begin{pmatrix}0 & v_n\\ v_n^{*} & 0\end{pmatrix}\begin{pmatrix}c_{n,1}\\ c_{n,2}\end{pmatrix}=\begin{pmatrix}c_{n,1}^{\dagger} & c_{n,2}^{\dagger}\end{pmatrix}U_n\begin{pmatrix}c_{n,1}\\ c_{n,2}\end{pmatrix}$$

$$c_n^{\dagger}H_{nn+1}c_{n+1}=\begin{pmatrix}c_{n,1}^{\dagger} & c_{n,2}^{\dagger}\end{pmatrix}\begin{pmatrix}0 & w_n\\ w_n^{*} & 0\end{pmatrix}\begin{pmatrix}c_{n+1,1}\\ c_{n+1,2}\end{pmatrix}=\begin{pmatrix}c_{n,1}^{\dagger} & c_{n,2}^{\dagger}\end{pmatrix}T_n\begin{pmatrix}c_{n+1,1}\\ c_{n+1,2}\end{pmatrix} \tag{46}$$

Using translational symmetry and Pauli matrices,

$$T_n=T,U_n=U$$

$$\sigma_x=\begin{pmatrix}0 & 1\\ 1 & 0\end{pmatrix},\sigma_y=\begin{pmatrix}0 & -i\\ i & 0\end{pmatrix},\sigma_z=\begin{pmatrix}1 & 0\\ 0 & -1\end{pmatrix} \tag{47}$$

We can construct the matrices T and U as:

$$U=\mathrm{Re}(v)\sigma_x-\mathrm{Im}(v)\sigma_y$$

$$T=\frac{1}{2}w\left(\sigma_x-i\sigma_y\right) \tag{48}$$

Using $\mathbf{c}_n = e^{ik(n-1)b}\mathbf{c}_1$, implies

$$\begin{aligned} &H = \oplus_{n=1}^{N} H(k) \quad \text{, with } H(k) = U + Te^{ikb} + T^{\dagger}e^{-ikb} = \mathbf{h}(k)\cdot\sigma \\ &h_x(k) = \mathrm{Re}(v) + |w|\cos\left(kb + \arg(w)\right) \\ &h_y(k) = -\mathrm{Im}(v) + |w|\sin\left(kb + \arg(w)\right) \\ &h_z(k) = 0 \end{aligned} \tag{49}$$

The eigenenergies are:

$$E(k) = \pm\sqrt{|v|^2 + |w|^2 + 2|v||w|\cos\left(kb + \arg(v) + \arg(w)\right)} \tag{50}$$

If $\arg(v) = \arg(w) = 0$, $v = w$ and $t_1 = v$ $t_2 = w$, we obtain the next figure:

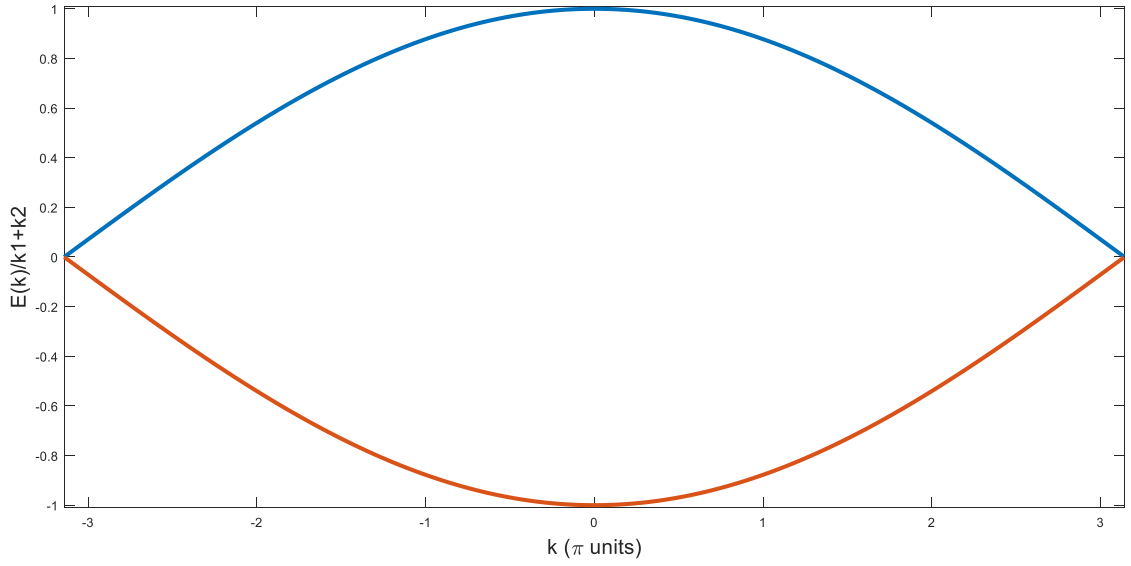

Figure 4. SSH model band structure with t1 ≠ t2.

Chapter 4

Topological effects in photonics lattices

Abstract

In this chapter some concepts of topology will be reviewed. In addition, we will study a one dimensional topological insulator, the SSH model.

Introduction

The discovering of topological phenomena in Physics, gave rise to develop the study of topological insulators. This systems are insulators in the bulk and are conductive on the surface through the edge states, like transportation channel, that were created in the material. Due to the tendency of miniaturization, the study of these edge states are important, as will be seen in the next section, the band structure of a material will be useful to determine its topological behavior.

4.1 Basics of Topology

Topology is the branch of mathematics that studies the quantities that are preserved under continuous deformations.

The quantities that remain constant under deformations are called topological invariants, these invariants help characterize different topologies. Objects with the same topological invariant are topologically equivalent, that means that they are in the same topological phase. There are many types of topological invariants, two examples are given below.

Figure 5 shows several geometries, which do not share the same topology with each other. The topological invariant that indicate their classification it is called genus, which corresponds to the number of holes in a closed surface. A topological phase transitions means when a hole is created or removed in the structure. If the genus is preserved, the surface can be deformed in its equivalent topology.

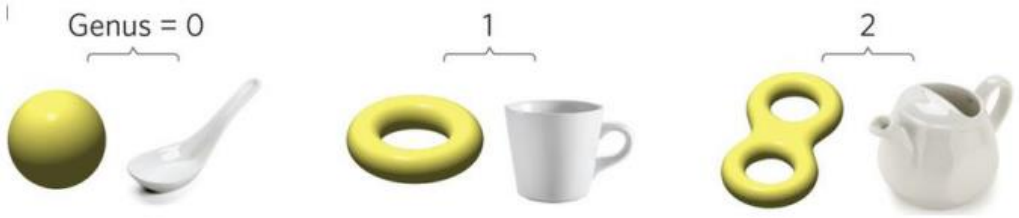

Figure 5. A spoon and a sphere share the same topological invariant (genus =0), just like the donut and the cup (genus=1)[7].

In physics, we will have that the band structure of a periodic array presents topological behavior, where the first Brillouin zone form a torus. Figure 6.

[7] Lu, Ling; Joannopoulos, John D.; Soljačić, Marin, "Topological Photonics", Nature Photonics, Volume 8, Issue 11, pp. 821-829 (2014).

The number of holes in this torus and the kind of closed paths will determine if the system is in the trivial or non-trivial classification.

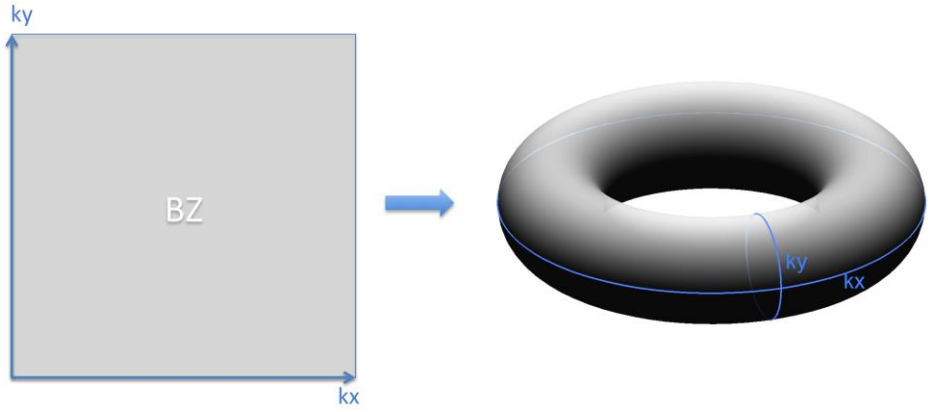

Figure 6. Torus of Brillouin. Geometrical relation between Brillouin zone and a torus.

4.2 Topological insulators.

A topological insulator is a physical system that presents topologically protected edge states at their boundaries due to a nontrivial topology of the bulk bands. This principle is called the bulk-boundary correspondence. We have that if bulk is nontrivial, topologically protected edge states appear at the boundaries, and conversely, topologically protected edge states are due to a nontrivial topology of bulk bands[8]. Using the concept of band energies, the properties of a topological insulator are shown schematically in the next figure.

[8] M Z Hasan and C L Kane 2010 Colloquium:Topological insulators Rev. Mod. Phys. 82 3045–3067

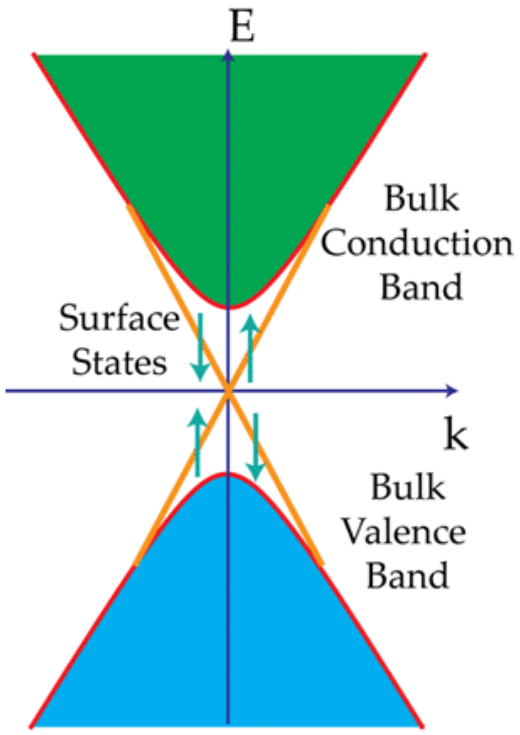

Figure 7. Topological insulator. The conducting occurs in the edge states of structure, when the bands meet in a Dirac Point.[9]

We can see that in a Topological insulator exists gapless edge states that allow conducting. In optics, the features of a topological insulator allow light to flow without dissipation around large imperfections in the structure[8].

In the torus, the trajectories of the edge states corresponds to closed paths that under deformations these will not be transformed into points, this only can occurs if the path is open.

The next figure shows two type of paths, we could see that the blue path that appears on the surface of the torus could be transformed in a point. In other hand, for the red path (edge states), we need to cut it. This means that

[9] William Berdanier: Photonic Topological Insulators, Building Topological States of Matter, B.S. Physics and B.S. Mathematics Thesis, Austin TX, (2013).

this path is protected under transformations.

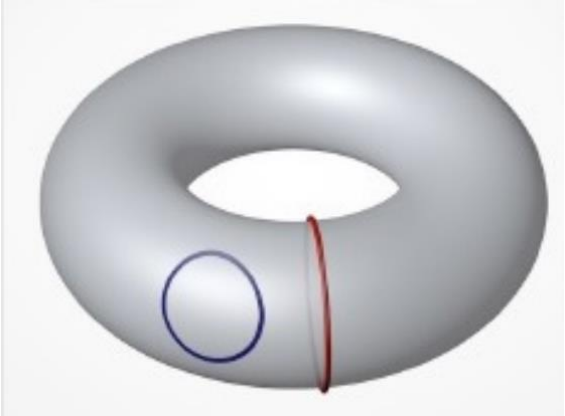

Figure 8. Closed paths in a topological insulator. The red path represents the edge states.

4.2.1 Topological insulator in 1D: SSH Model

The SSH model is the most important one dimensional topological insulators. To study the topological properties of this model, we will use the equation (50): $E(k) = \pm\sqrt{|v|^2 + |w|^2 + 2|v||w|\cos(kb + \arg(v) + \arg(w))}$

Considering arg (v) = 0, kb = [-π, π], we have two cases (Figure 9):

1)

2)

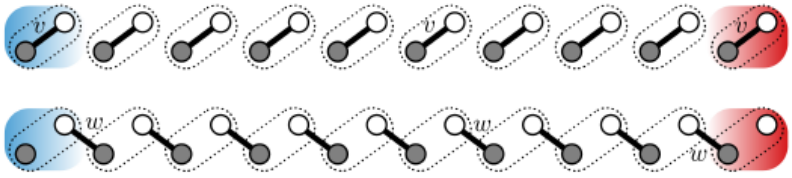

Figure 9. SSH Model with different interactions between the particles.

The Topological phases are given as:

- Case 1. |v|>|w| Trivial Topological transition.
- Case 2. |w|>|v| Non Trivial Topological transition.

The topological transition obtained of SSH model is shown in the next figures. The energies of the Figure 10, 11 and 13 are staggered. The Figure 12 shows the SSH model as a conductor, this represents the transition point between the Figure 11 and 13.

The Figure 11 shows the trivial topological transition. We can see that after the change in the hopping amplitudes, the bands presents an inversion shown in the figure 13, this corresponds to the Non Trivial topological transition.

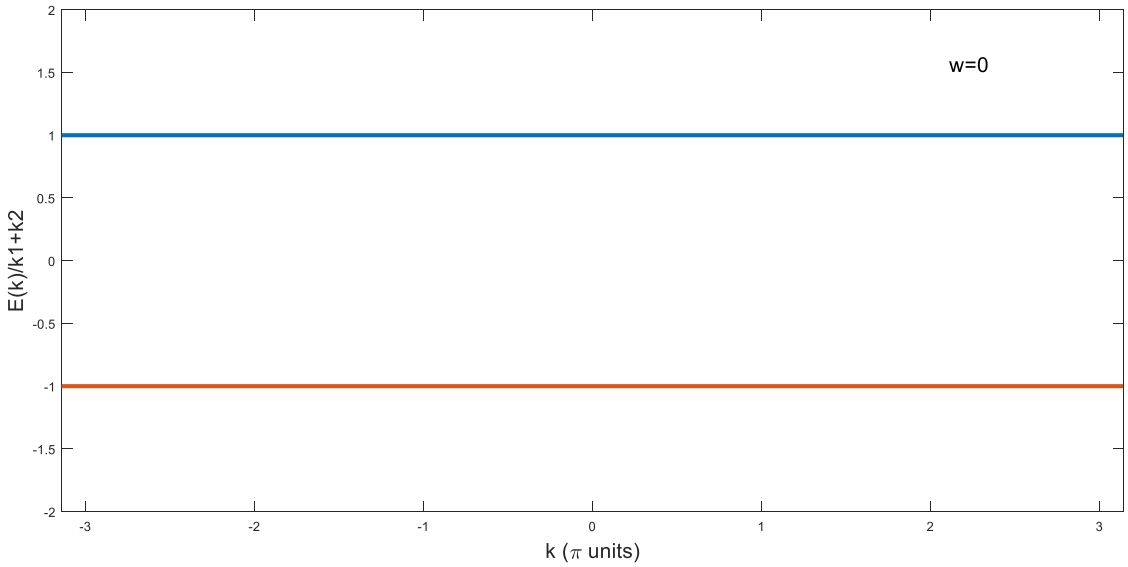

Figure 10. Band structure for w=0 (similar figure is obtained with v=0).

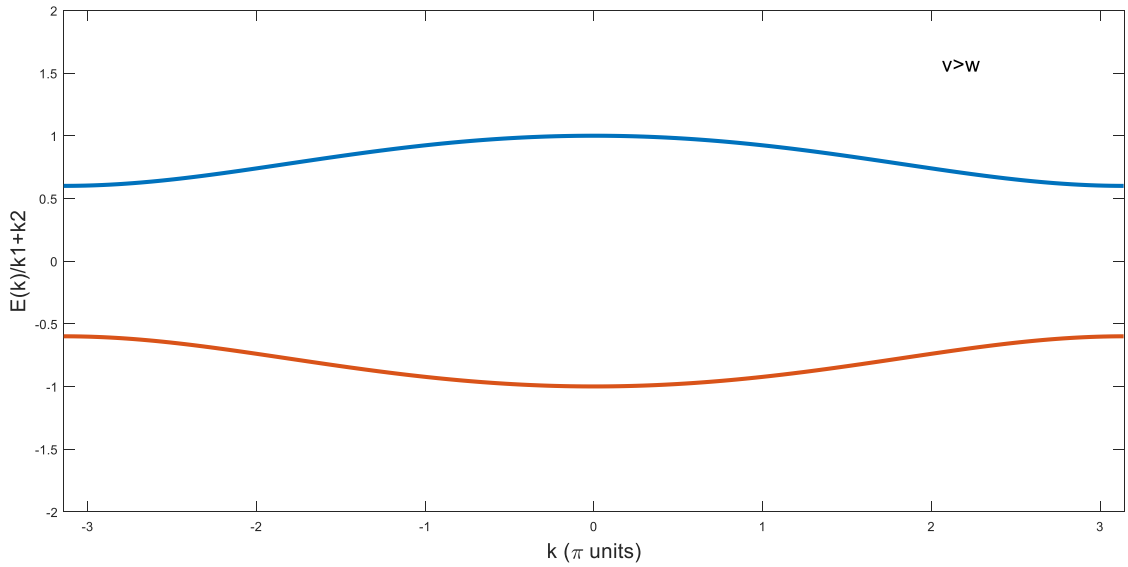

Figure 11. Band structure for v>w. Topological Trivial phase.

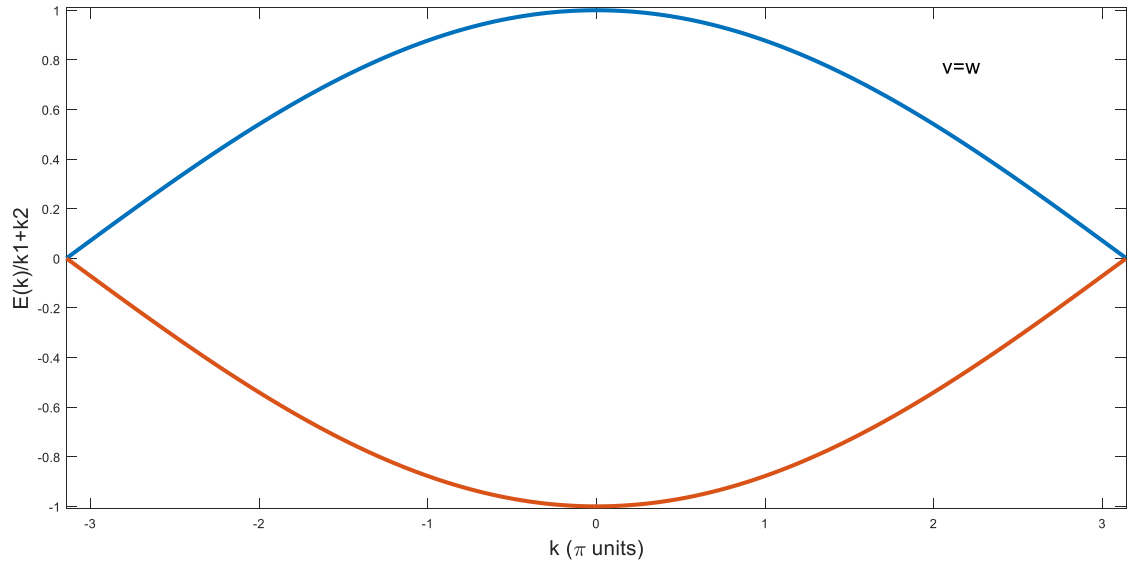

Figure 12. Band structure for v=w. Phase boundary.

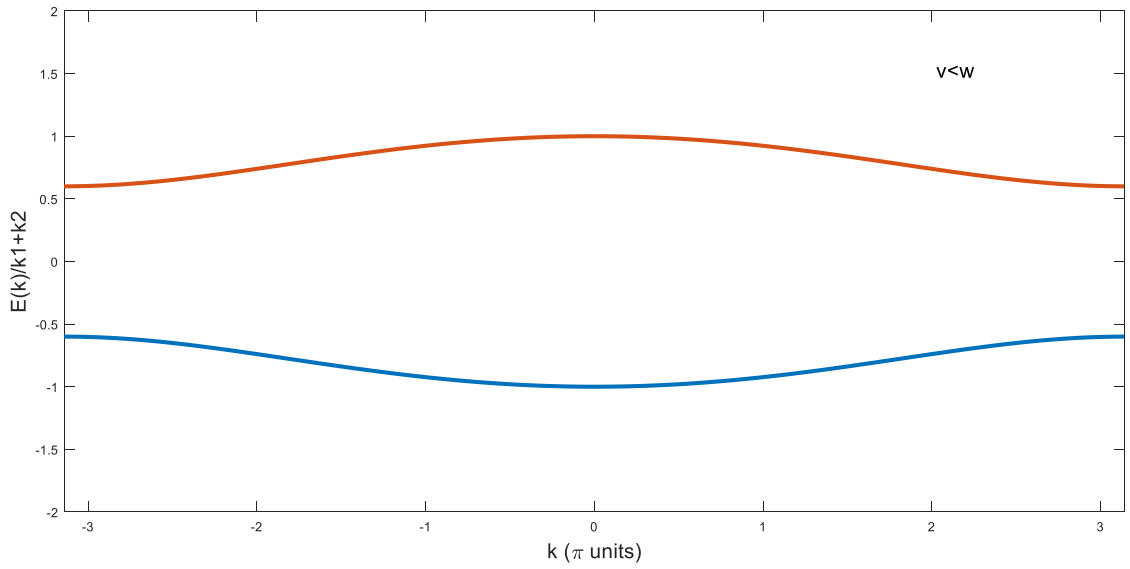

Figure 13. Band structure for v<w. Non-Topological Trivial phase.

CHAPTER 5

Non-Hermitian Topological Photonics. Numerical analysis.

Abstract

Recent works have suggested PT symmetric versions of SSH model in optical settings, demonstrating the existence of edge states and developing the study of topological Non-Hermitian systems[10][11][12].

In this chapter we will show the conditions to have an Optical PT system. Then, we study an Optical PT system made of two coupled microrings resonators. The designed has refractive index n = 3.18. The unbroken and broken PT phases for this system were obtained by COMSOL simulations.

Finally, the properties of an SSH array generated by a periodic and finite coupled pairs of PT microring resonators, proposed by M.Parto and et.al.[13], will be analyzed.

[10] J. M. Zeuner, M. C. Rechtsman, Y. Plotnik, Y. Lumer, S. Nolte, M. S. Rudner, M. Segev, and A. Szameit, Phys. Rev. Lett. 115, 040402 (2015).
[11] A.Weimann, M. Kremer, Y. Plotnik, Y. Lumer, S. Nolte, K. Makris, M. Segev, M. Rechtsman, and A. Szameit, Nature materials 16, 433 (2017).
[12] L. Xiao, X. Zhan, Z. H. Bian, K. K. Wang, X. Zhang,X. P. Wang, J. Li, K. Mochizuki, D. Kim, N. Kawakami,
and et al., Nature Physics 13, 11171123 (2017).
[13] M. Parto, S. Wittek, H. Hodaei, G. Harari, M. A. Bandres, J. Ren, M. C. Rechtsman, M. Segev, D. N. Christodoulides, and M. Khajavikhan, Phys. Rev. Lett. 120, 113901 (2018)

5.1 PT symmetry in Optics

Considering the Helmholtz equation for a field $E(x,z)$:

$$\frac{\partial^2}{\partial x^2}E(x,z)+\frac{\partial^2 E(x,z)}{\partial z^2}+k_0^2 n^2 E(x,z)=0 \tag{51}$$

Where $k_0=\frac{2\pi}{\lambda_0}, n$ is the substrate index. Taking into account the paraxial regime, we can write:

$$E(x,z)=\tilde{E}(x,z)\mathrm{e}^{ik_0 n_0 z} \tag{52}$$

The variations of z are much smaller than the variations in x, because of that we can neglect the second order derivatives respect to z.

$$-\frac{1}{2k_0^2 n_0}\frac{\partial^2\tilde{E}}{\partial x^2}+\Delta n\tilde{E}=\frac{i}{k_0}\frac{\partial\tilde{E}}{\partial z} \tag{53}$$

But, we will use a z independent refraction index, this allows to write $\Delta n = n$ and taking into account the real and imaginary part of the refraction index, we obtain:

$$i\frac{\partial\tilde{E}}{\partial z}=-\frac{1}{2k_0 n_0}\frac{\partial^2\tilde{E}}{\partial x^2}+k_0 n\tilde{E} \tag{54}$$

$$i\frac{\partial\tilde{E}}{\partial z}=-\frac{1}{2k_0 n_0}\frac{\partial^2\tilde{E}}{\partial x^2}+k_0\left[n_R(x)+in_I(x)\right]\tilde{E} \tag{55}$$

The equation 55 is called the paraxial equation and a relation between the Schrödinger wave equation has been established[14]:

$$i\frac{\partial \tilde{E}}{\partial z} = -\frac{1}{2k_0 n_0}\frac{\partial^2 \tilde{E}}{\partial x^2} + k_0\left[n_R(x) + in_I(x)\right]\tilde{E} \Leftrightarrow i\hbar\frac{\partial \psi}{\partial t} = -\frac{\hbar^2}{2m}\frac{\partial^2 \psi}{\partial x^2} + V(x)\psi \qquad (56)$$

This has allowed to establish the relationship between the complex potential and the refractive index, i.e. $V(x) = k_0\left(n_R(x) + in_I(x)\right)$, generating the creation of new materials inspired by the concepts of PT symmetry theory and the discovery of many applications. Due the condition $V(\hat{x}) = V^*(-\hat{x})$ (equation 33), PT-symmetry in optics demands the following properties:

- $\left(n_R(x) = n_R(-x)\right)$: The spatial distribution of the refractive index is an even function of the space.
- $\left(n_I(x) = -n_I(-x)\right)$: The imaginary component representing gain or loss, is an odd function of position and their value not affect the real part of refractive index. The PT symmetry condition could be expressed with the complex permittivity as $\varepsilon(r) = \varepsilon^*(-r)$.
- The spatial evolution along z is analog to the temporal evolution of the wave function. In this analogy the effect of the time reversal operator will correspond to the change in the direction of propagation z.

We can model an optical PT system through two coupled microring resonators, this system will be described in the next section.

[14] R. El-Ganainy, K. G. Makris, D. N. Christodoulides, and Ziad H. Musslimani, "Theory of coupled optical PT-symmetric structures," Opt. Lett. 32, 2632-2634 (2007)

5.2 Optical microring resonators

An optical ring resonator can be viewed like a closed loop optical waveguide, this confines light in all spatial directions, light propagating in the ring resonator interferes with itself after every trip around the ring. When the roundtrip length is exactly equal to an integer multiple of the guided wavelength, constructive interference occurs.

Ring resonators are one of the most versatile photonic devices, due to their high miniaturization (as a microrings resonators), high wavelength selectivity, large field enhancement, and high quality factor. These features have turned microrings into devices used in different areas, such as optical communication, signal processing, sensing, nonlinear optics and quantum optics.

Recently, the microring resonators have been used to demonstrate PT symmetry in Optics[15].

5.2.1 Optical ring resonator theory

Figure 14 shows the most used and investigated ring resonators. The coupling of the light is achieved as follows, a fraction of the wave E_{i1} is transmitted in the straight waveguide while the other fraction (E_{t2}) is coupled to the ring. Part of the wave coupled to the ring (E_{i2}) is coupled to the straight waveguide becoming the E_{t1} wave, while the rest of that wave continues around the waveguide of the ring. Where t is the transmission coefficient, κ is the coupling coefficient and α is the round-trip loss.

[15] H. Hodaei, et al., "Parity-Time-Symmetric Microring Lasers," Science **346**, 975 (2014).

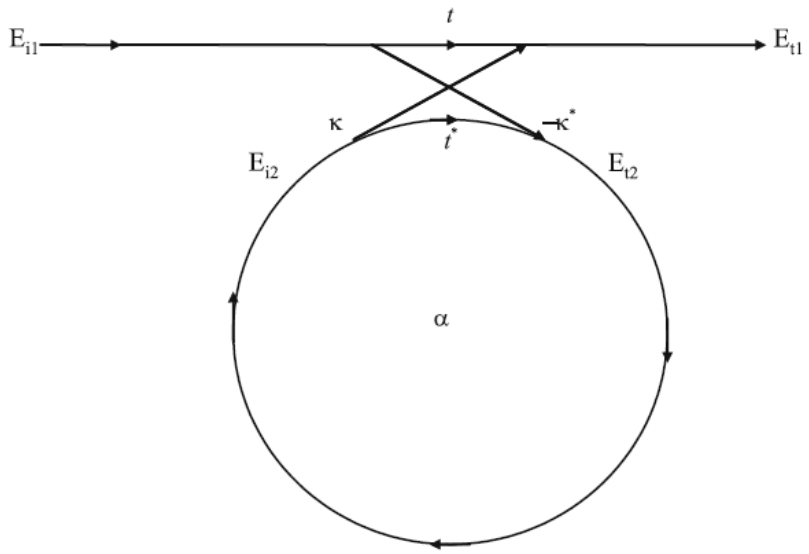

Figure 14. Optical ring resonator coupled with a linear waveguide[16].

The fields are related by the following matrix relation[15]:

$$\begin{pmatrix} E_{t1} \\ E_{t2} \end{pmatrix} = \begin{pmatrix} t & \kappa \\ -\kappa^* & t^* \end{pmatrix} \begin{pmatrix} E_{i1} \\ E_{i2} \end{pmatrix} \tag{57}$$

With:

$$\left|E_{t1}\right|^2 + \left|E_{t2}\right|^2 = \left|E_{i1}\right|^2 + \left|E_{i2}\right|^2 \tag{58}$$

$$\left|t\right|^2 + \left|\kappa\right|^2 = 1 \tag{59}$$

Choosing E_{i1} = 1. The wave propagates around the ring, with radius R, with accumulated phase ϕ=kR, the relationship is given by:

$$E_{i2} = \alpha e^{j\phi} E_{t2} \tag{60}$$

For a lossless ring α=1, we have that each value of ϕ= 0, 1,2,…, will specify the resonance modes of the ring.

[16] D.G Rabus, "Integrated Ring Resonators, The Compendium", Springer, 2007.

Another parameter is the propagation constant, defined by:

$$\beta = \frac{2\pi n_{eff}}{\lambda} \tag{61}$$

where n_{eff} is the refractive effective index.

The electric and magnetic field for the light in the ring could be expressed considering a dielectric waveguide or radius R, with refractive index n and constant of propagation β, Electric and Magnetic field distribution are given as:

$$\begin{aligned} \boldsymbol{\mathcal{E}} &= \mathbf{E} e^{-i\beta\phi} \\ \boldsymbol{\mathcal{H}} &= \mathbf{H} e^{-i\beta\phi} \end{aligned} \tag{62}$$

The fields **E** and **H** satisfy Maxwell's equations:

$$\begin{aligned} \nabla \times \boldsymbol{\mathcal{E}} &= -i\omega\mu_0 \boldsymbol{\mathcal{H}} \\ \nabla \times \boldsymbol{\mathcal{H}} &= i\omega\varepsilon_0 n^2 \boldsymbol{\mathcal{E}} \end{aligned} \tag{63}$$

where ε_0 and μ_0 are the electric permittivity and magnetic permeability of vacuum, respectively.

Eliminating the cross product of the second equation, we obtain:

$$\nabla \times \nabla \times \boldsymbol{\mathcal{E}} = n^2 k^2 \boldsymbol{\mathcal{E}} \tag{64}$$

where $k = \omega / c$.

The obtained equation represents an eigenvalue problem, whose solutions give the distribution of the field $\mathbf{E}$ of each mode with propagation β.

The solution of the equation (64) can be found with the Finite Element Method, in this work this method was used through COMSOL software.

5.2.2 Microring resonator eigenfrequencies

Figure 15 shows the simulation of whispering gallery modes supported by a single microring resonator. The microrings used in the simulation have a radii of 10 μm, width of 1.55 μm, refractive index n=3.18 and the rings are covered by air (n=1.0).

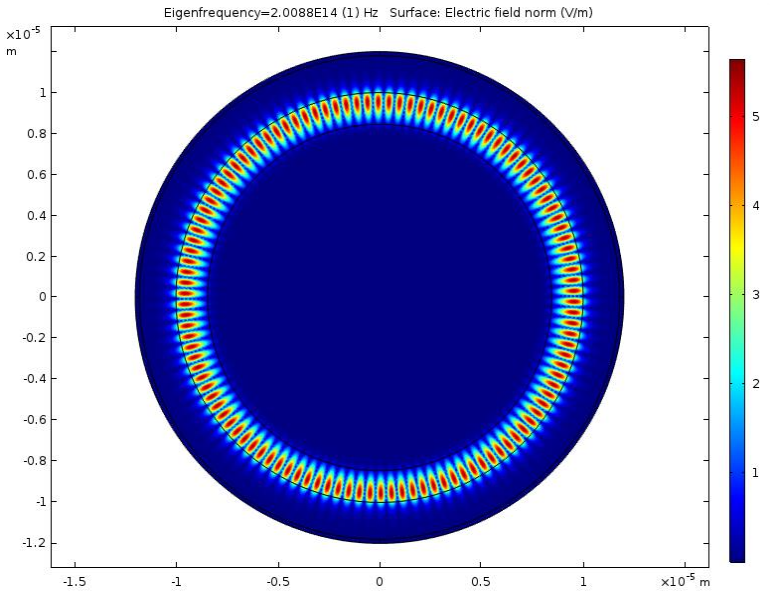

Figure 15. Electric field intensity of microring. 2D simulation.

5.2.3 PT symmetry breaking in coupled microring resonators

An optical PT system can be realized by two coupled microrings, where one cavity provides gain and the other cavity loss. This system must satisfy the following conditions: $\left(n_R(x) = n_R(-x)\right)$ and $\left(n_I(x) = -n_I(-x)\right)$.

When two resonators are coupled, they obey the differential equations for their modal amplitudes a, b, clockwise and anticlockwise respectively:

$$\begin{aligned} \frac{da}{dt} &= -i\omega a + \gamma_a a \; + i\kappa b \\ &\text{Eigenfrecuency + Gain/Loss + Coupling} \\ \frac{db}{dt} &= -i\omega b + \gamma_b b \; + i\kappa a \end{aligned} \tag{65}$$

Where γ coefficient represents the imaginary part of refractive index, whose sign determines if we have gain or loss. The model used was taken of H. Hodaei, et al.[15]

The matrix form of the system is:

$$i\frac{d}{dt}\begin{pmatrix} a \\ b \end{pmatrix} = \begin{pmatrix} \omega + i\gamma_a & -k \\ -k & \omega + i\gamma_b \end{pmatrix}\begin{pmatrix} a \\ b \end{pmatrix} \tag{66}$$

We have that Hamiltonian is not Hermitian. To verify if is PT symmetric, we take into account the condition (31):

$$\hat{P}\hat{T}\hat{H} = \hat{H}\hat{P}\hat{T} \tag{67}$$

Applying (67) with $\hat{P} = \begin{pmatrix} 0 & 1 \\ 1 & 0 \end{pmatrix}$ and T the complex conjugation:

$$\hat{P}\hat{T}\hat{H} = \begin{pmatrix} -k & \omega - i\gamma_b \\ \omega - i\gamma_a & -k \end{pmatrix} = \hat{H}\hat{P}\hat{T} \tag{68}$$

The result obtained in (68) shows that the system is PT symmetric.

The eigenfrecuencies ω' of the system are:

$$\omega' = \omega + i\frac{\gamma_a + \gamma_b}{2} \pm \sqrt{\kappa^2 - \left(\frac{\gamma_a - \gamma_b}{2}\right)^2} \tag{69}$$

With the PT condition $\gamma_a = -\gamma_b \equiv \gamma_n$ (one of the ring is subject to gain while the other one is subject to the same amount of loss), the equation simplifies to:

$$\omega' = \omega \pm \sqrt{\kappa^2 - \gamma_n^2} \tag{70}$$

An exceptional point (the transition point between unbroken and broken phase) is found if $|\gamma_n| = \kappa$.

The PT symmetry will be unbroken if $|\gamma_n| < \kappa$. When the gain-loss contrast between the rings exceeds the strength of coupling, $|\gamma_n| > \kappa$, we will have the broken PT phase. For a spacing of 200nm, Figure 16 shows the unbroken PT phase and Figure 17 shows the broken PT phase, obtained with n_i=0.004.

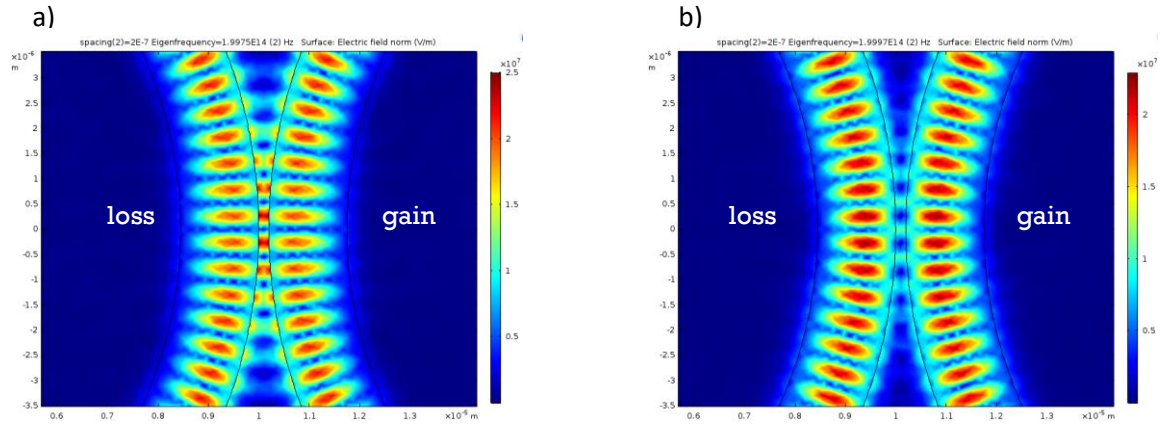

Figure 16.Unbroken PT phase/ spacing 200nm. Supermode 1 (left) and supermode 2 (right).

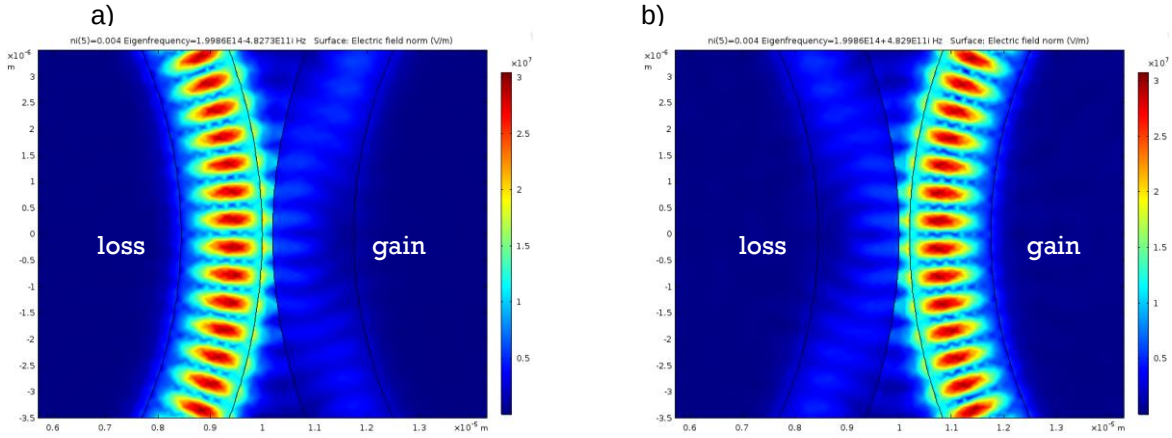

Figure 17.Broken PT phase/ spacing 200nm.

Simulations were designed to obtain modes around 1550nm. The spacing of 200nm was chosen after having done a spacing sweep (100nm to 400nm), in this spacing the frequencies showed more clearly. Figure 18 shows the images obtained of spacing sweep.

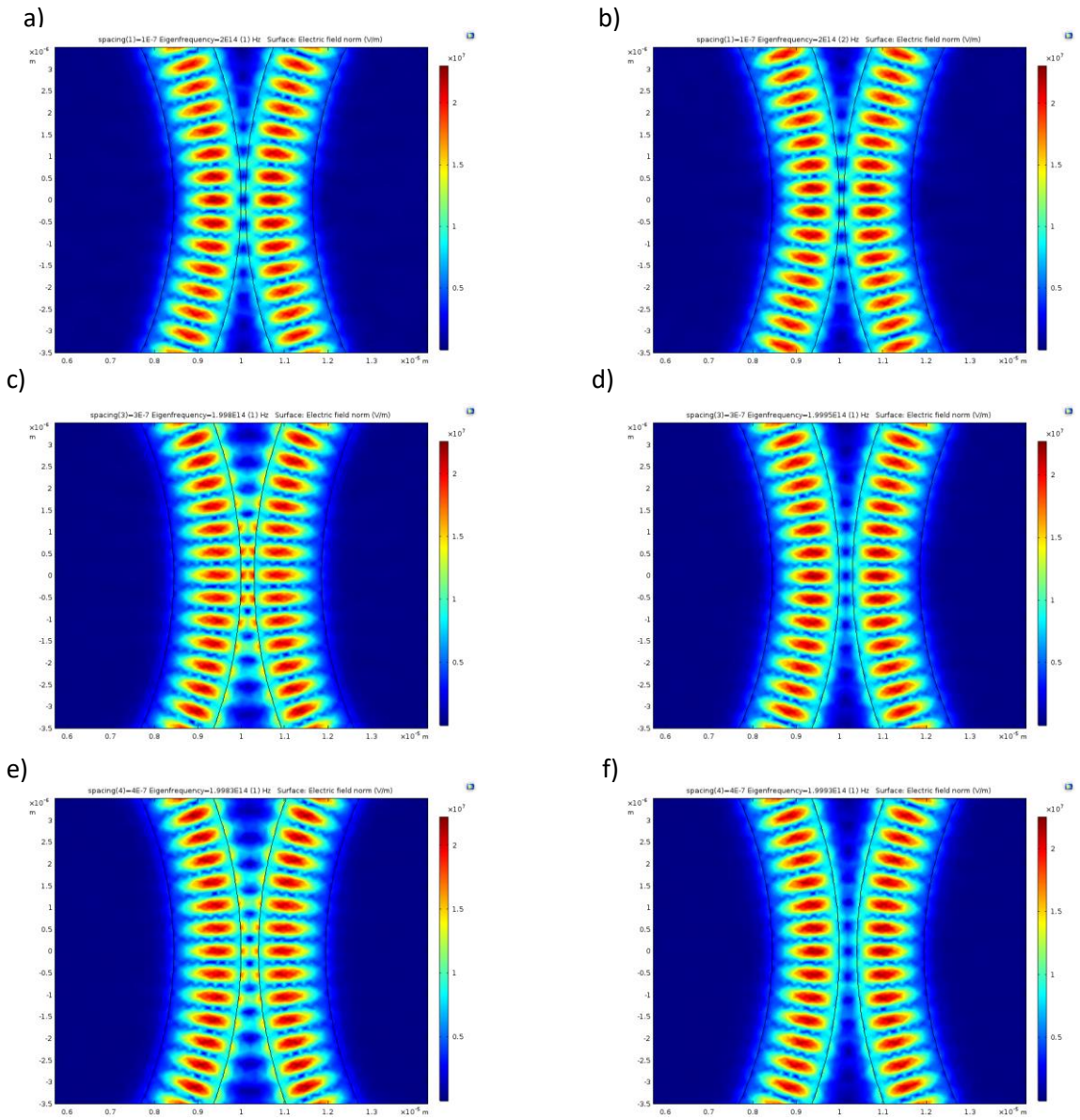

Figure 18. Spacing sweep of 100nm, 300nm and 400nm respectively.

5.3 SSH Microring array

We have a SSH microring array, Figure 19.

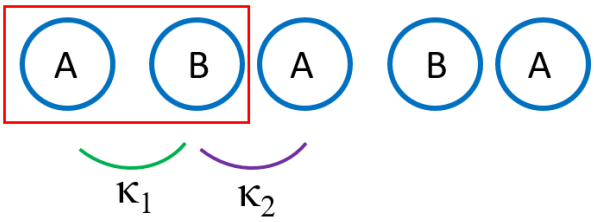

Figure 19. SSH microring array.[13]

The microrings A and B are microrings resonators. As we can see, the array have a nontrivial termination.

The dynamics of this array can be seen as the sum of a single SSH lattice with κ_1 and κ_2 are the couplings between the lattices and ε_A and ε_B are the potentials.

The Hamiltonian of the model is[13]:

$$H_0 = \varepsilon_A \sum_n c_n^{A\dagger} c_n^A + \varepsilon_B \sum_n c_n^{B\dagger} c_n^B + \sum_n \left[\kappa_1 \left(c_n^{B\dagger} c_n^A + c_n^{A\dagger} c_n^B \right) + \kappa_2 \left(c_{n-1}^{B\dagger} c_n^A + c_n^{A\dagger} c_{n-1}^B \right) \right] \quad (71)$$

Using translational symmetry:

$$c_{n+R} = c_n e^{ikR} \Rightarrow c_{n-1}^B = c_n^B e^{-ik} \quad (72)$$

We have:

$$H_0 = \varepsilon_A \sum_n c_n^{A\dagger} c_n^A + \varepsilon_B \sum_n c_n^{B\dagger} c_n^B + \sum_n \left[\kappa_1 \left(c_n^{B\dagger} c_n^A + c_n^{A\dagger} c_n^B \right) + \kappa_2 \left(c_n^{B\dagger} c_n^A e^{ik} + c_n^{A\dagger} c_n^B e^{-ik} \right) \right] \quad (73)$$

Writing in the form $\begin{pmatrix} c_n^{A\dagger} & c_n^{B\dagger} \end{pmatrix} (H_0) \begin{pmatrix} c_n^A \\ c_n^B \end{pmatrix}$

We obtain the Hamiltonian:

$$H_0 = \begin{pmatrix} \varepsilon_A & \kappa_1 + \kappa_2 e^{-ik} \\ \kappa_1 + \kappa_2 e^{ik} & \varepsilon_B \end{pmatrix} \tag{74}$$

From this Hamiltonian we can have the following cases:

- Case I. $\varepsilon_A = \varepsilon_B = 0$ (Potential =0). Hermitian case.

If we set the potentials of the microrings equal to zero, we obtain that the SSH system will be Hermitian and the eigenvalues of the Hamiltonian are:

$$E = \pm\sqrt{\kappa_1^2 + \kappa_2^2 + 2\kappa_1\kappa_2 \cos(k)} \tag{75}$$

Evidently the Hamiltonian is Hermitian:

$$H_0{}^{\dagger} = \begin{pmatrix} 0 & \kappa_1 + \kappa_2 e^{-ik} \\ \kappa_1 + \kappa_2 e^{ik} & 0 \end{pmatrix} \tag{76}$$

- Case II. $\varepsilon_A = g = \varepsilon_B$

If we set the potentials of the microrings as identical, g, the same case as the Hermitian will be obtained.

Therefore, we have that the eigenvalues are given as:

$$H_0 = \begin{pmatrix} g & \rho \\ \rho^* & g \end{pmatrix} \text{ with } \rho = \kappa_1 + \kappa_2 e^{-ik} \tag{77}$$

Where the eigenvalues appear shifted by -ig in their imaginary part:

$$E = g \pm \sqrt{|\rho|^2} \tag{78}$$

Figure 20 shows the band structure for Case I and II.

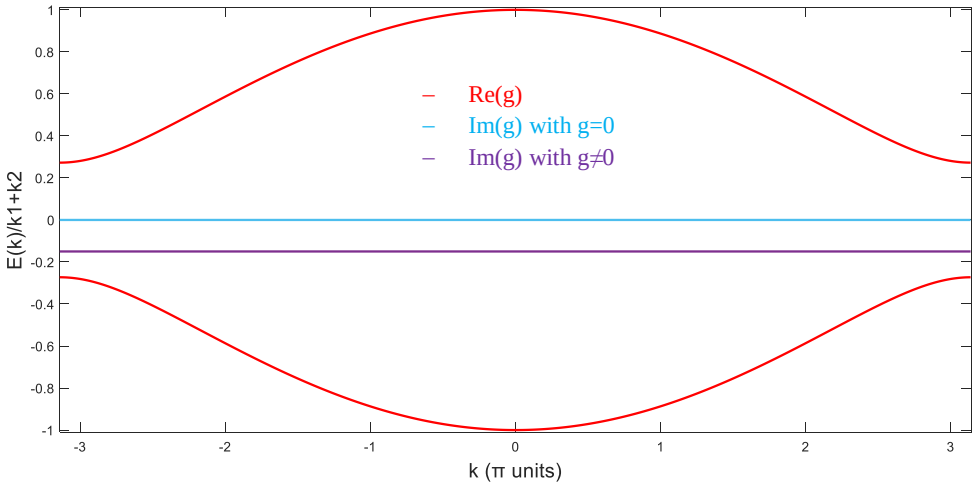

Figure 20. Real and Imaginary part of Case I and II.

– Case III. $\varepsilon_A = -ig = \varepsilon_B$, active SSH array.

If the structure is active, it means that the potentials are purely imaginary, we have:

$$H_0 = \begin{pmatrix} -ig & \rho \\ \rho^* & -ig \end{pmatrix} \tag{79}$$

5.3.1 Active SSH array with PT symmetry

When the PT symmetry is introduced in the system, under this condition, the microrings must have identical but opposite complex potentials.

That implies that the Hamiltonian will be:

$$H_0 = \begin{pmatrix} -ig & \rho \\ \rho^* & +ig \end{pmatrix} \tag{80}$$

Where the eigenvalues are:

$$E = \pm\sqrt{|\rho|^2 - g^2} \tag{81}$$

To observe the topological behavior of the PT symmetry phases in the system, the following variables are introduced[13]:

$$\nu = \frac{\kappa_2}{\kappa_1} \qquad \eta = \frac{g}{\kappa_1} \tag{82}$$

Where ν corresponds to the dimerization, which gives the parameter to place in the edge of the array.

The variable η corresponds to the normalized gain and loss, which will indicate the transition of the PT symmetry phase.

Therefore, the eigenvalues are:

$$E = \pm\kappa_1\sqrt{1+\nu^2+2\nu\cos(k)-\eta^2} \tag{83}$$

For this simulation we assume $\nu = 2$.

We have the next phases in the array:

- $0 < \eta < \nu - 1$ with $\eta = 0.06$

We obtain the band structure shown in figure 21.

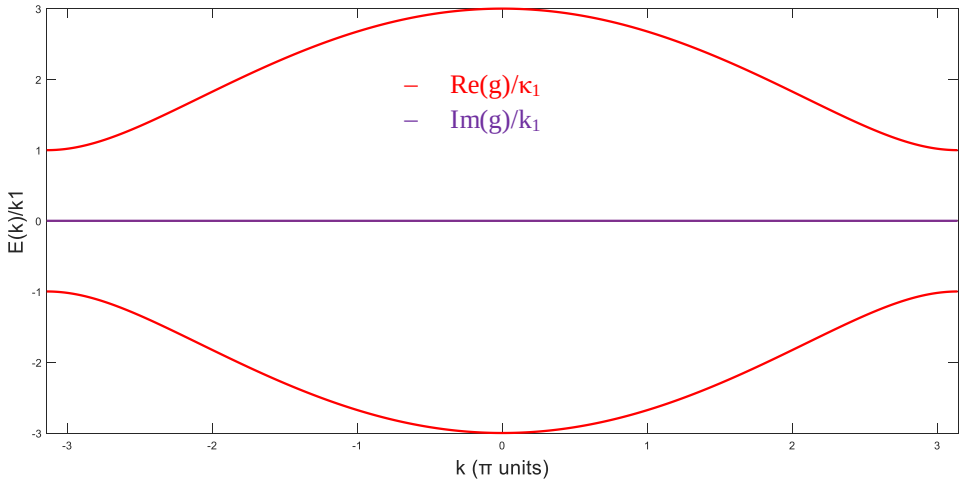

Figure 21. PT symmetric SSH model, $0 < \eta < \nu - 1$.

– $\nu - 1 < \eta < \nu + 1$ *with* $\eta = 1.1$

The gain value increased, we have PT symmetry broken phase. Figure 22 shows that the eigenvalues became complex.

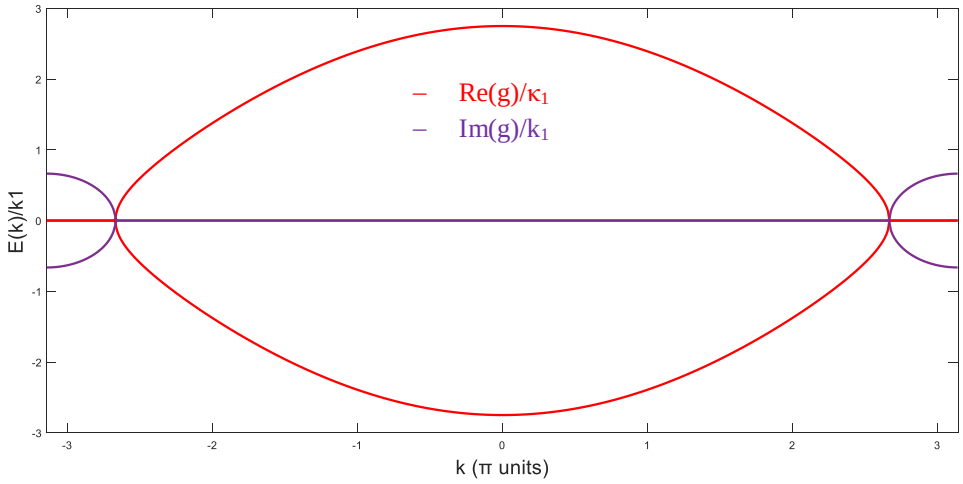

Figure 22. PT symmetric SSH model, transition phase.

– $\eta > \nu + 1$ *with* $\eta = 3.1$

In this phase the PT symmetry is totally broken, because the high contrast between gain and loss, all eigenvalues are complex. Figure 23.

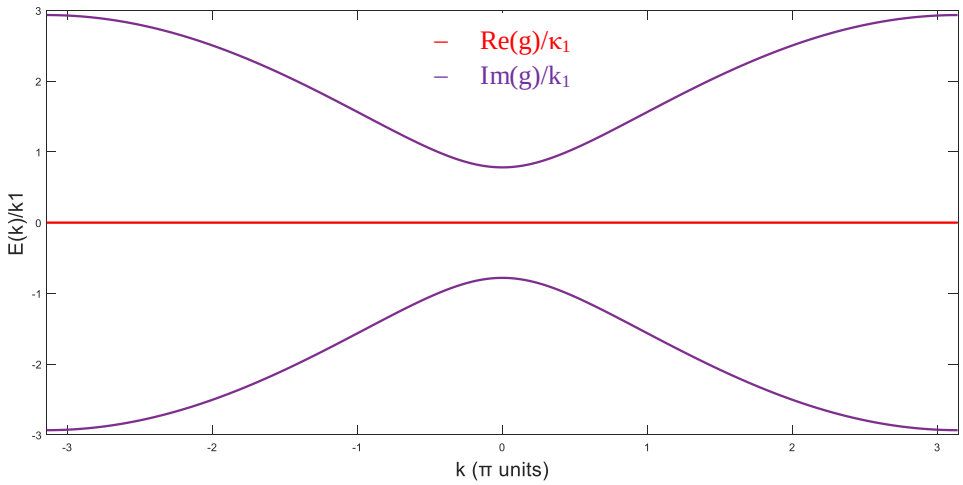

Figure 23. PT symmetric SSH model, $\eta > \nu + 1$

Chapter 6

Conclusions

In this work, a PT symmetric system made by two coupled micro rings was studied. This model can be applied to other semiconductor materials. In this work, a predefined model was used, with n = 3.18.

The goal of the first part of the work was to analyze the behavior of PT symmetry. From the simulations obtained, Figure 16 showed the phase where the PT symmetric conditions are satisfied. It was observed that both rings show resonance.

Figure 17 shows the phase where the PT symmetry is completely broken. As the symmetry breaks, the ring modes compete until finally only one show the total amplification.

The objective of the final part was the study of PT symmetry in an SSH array, through the coupled microring resonators.

The phase III of this system, the PT symmetric phases were observed.

Figure 21 shows the phase where the PT symmetry is satisfied in the active SSH array. The eigenvalues are completely real.

Subsequently, the gain was increased, figure 22 shows that the eigenvalues of the system became imaginary.

Figure 23 shows the phase of broken PT symmetry, we can see that the spectrum of eigenvalues became purely imaginary. The system is in the non-trivial topological phase.

Because symmetries play an important role to defining the topology, as a future work we will study the symmetries of the system, through the symmetry-protected topological phase classification[17].

In addition, we will obtain the number of edge states of the system and we will study the relation with the PT symmetry. Because the final system is Non-Hermitian, we will obtain the complex Berry phase to corroborate the values of each phase of the PT-active SSH array system.

Finally, the intensities of the modes will be obtained, in order to study the emission properties under topological protection.

[17] A. P. Schnyder, S. Ryu, A. Furusaki, and A. W. W. Ludwig, Phys. Rev. B 78, 195125 (2008)